Optica Applicata, Vol. XXXIX, No. 4, 2009

(100) GaAs surface treatment prior to contact metal deposition in AlGaAs/GaAs quantum cascade laser processing

EWA PAPIS[1*], ANNA BARAŃSKA[1], PIOTR KARBOWNIK[1], ANNA SZERLING[1], ANNA WÓJCIK-JEDLIŃSKA[1], MACIEJ BUGAJSKI[1], WITOLD RZODKIEWICZ[1], JACEK SZADE[2], ANDRZEJ WAWRO[3]

[1]Institute of Electron Technology, al. Lotników 32/46, 02-668 Warsaw, Poland

[2]Institute of Physics, University of Silesia, Uniwersytecka 4, 40-007 Katowice, Poland

[3]Insitute of Physics PAS, al. Lotników 32/46, 02-668 Warsaw, Poland

[*]Corresponding author: papis@ite.waw.pl

The effects of HCl-based chemical and Ar^+ sputter etching treatment on (100) GaAs surface properties with the aim to develop the procedure of surface preparation before metal deposition have been investigated. Variable angle spectroscopic ellipsometry, X-ray photoelectron spectroscopy, atomic force microscopy and photoluminescence have been used to study the surface characterization. We show that combining chemical etching in 5% HCl with Ar^+ sputter etching gives the best results for surface cleaning prior to metal deposition. The application of this two-step treatment allows to obtain Ni/AuGe/Ni/Au ohmic contact with $r_c = 2\times10^{-6}$ Ωcm^2 with excellent adhesion and long-term thermal stability.

Keywords: GaAs, surface treatment, sputter etching.

1. Introduction

GaAs and related materials are well recognized for their potential application in modern micro- and optoelectronic devices. GaAs-based layered heterostructures are very suitable for obtaining high-performance semiconductor lasers, in particular AlGaAs/GaAs quantum cascade lasers (QCLs), which are very attractive sources for many laser-based applications areas, such as medicine, chemical sensing, molecular spectroscopy and free-space communication [1–3]. Specific layered construction of QCLs requires high quality of surface with good morphology and controlled composition, properties that depend on surface pre-treatment before metal deposition during formation of ohmic contact. One of the feasible ways is sputter etching in Ar^+ plasma, which would be an effective and promising method of *in-situ* surface

preparation prior to metal deposition if ion-induced damage of semiconductor surface could be minimized [4]. A complete understanding of the mechanism of the surface damage is very important for QCL processing. Several researchers have reported investigations of the damaged layer induced by ion etching [5, 6]. It has been found that sputter etching introduced both discrete and continuous level defects in *n*-type GaAs. These defects decreased the barrier height of Schootky barrier diodes [6]. It is well known that GaAs surface characterised a high surface energy and as a consequence it is very reactive and chemically unstable. Due to the reactivity of the native oxides, it is difficult to perform the analysis of GaAs surface chemical composition. Low energy Ar^+ ion etching has been widely used for sputter cleaning, despite the evidence that ion bombardment can modify not only the surface morphology and structure but also the surface composition [7, 8]. In this paper, the effects of wet chemical and Ar^+ sputter etching on (100) GaAs surface were comprehensively investigated by spectroscopic ellipsometry (SE), X-ray photoelectron spectroscopy (XPS), atomic force microscopy (AFM) and additionally photoluminescence (PL). Finally, a practical application of the Ar^+ plasma etching for *in-situ* surface preparation prior to Ni/AuGe/Ni/Au ohmic contact deposition was demonstrated.

We show that the two-step treatment combining chemical etching in 5% HCl with Ar^+ sputter etching gives the best results for surface cleaning prior to metal deposition.

2. Experiment

The GaAs samples used in these experiments were (100) oriented monocrystalline wafers doped Si to the concentration of $n = 2\times10^{18}$ cm^{-3}. Prior to experiments the samples received standard surface cleaning consisting in decreasing in hot organic solvents. Complementary research has been carried out on Ar^+ sputter etching in Leybold L400sp system in which further processes of metallic Ni/AuGe/Ni/Au (5/100/35/300 nm) structures deposition are carried. The samples were annealed in rapid thermal annealing (RTA) system at the temperature $T = 450$ °C. Long-term thermal stability was investigated by annealing samples in a gas-flow furnace at the temperature $T = 200$ °C for 16 h.

Three procedures of surface pre-treatment have been compared: *i*) wet chemical etching in 5% HCl for 60 s at RT, *ii*) sputter etching in Ar^+ plasma performed directly before metallic layers deposition, *iii*) two steps treatment: etching in 5% HCl for 60 s at RT followed by sputter etching in Ar^+ plasma. Sputter etching was performed in Ar^+ plasma at working pressure of $p = 3\times10^{-3}$ mbar, gas flow of $f_{Ar^+} = 100$ sccm, power P and time etching t varied in the range 70–250 W and 20–90 s, respectively. Woollam variable angle spectroscopic ellipsometer (VASE) was chosen to provide complementary information on the thickness, refractive index and extinction coefficient of modified surface films. Ellipsometric analysis was performed in the spectral range 240–1100 nm at two angles 65° and 75°. To extract physical information from VASE date, two bilayer models were performed. The first is GaAs oxide layer on GaAs substrate and the second one is modified GaAs superficial layer

on GaAs substrate. Modified GaAs superficial layer means that refractive index and extinction coefficient of GaAs have been changed and fitted during ellipsometric analyses [9].

The chemistry and electronic structure of the prepared surface was analyzed by XPS using a PHI 5700 spectrometer from Physical Electronics. Monochromatized Al K_α radiation and the analysis angle of 45° were used. The spectral line of C 1s (E_B = 284.6 eV) was used to calibrate the binding energy. The XPS database from Physical Electronics Handbook of Photoelectron Spectroscopy [10] and NIST database were applied as the preliminary reference for identifying the chemical states of elements. The MULTIPAK software from Physical Electronics was applied to deconvolute the XPS spectra. The Shirley background and Gaussian convoluted with Lorentzian lines were used in the fitting procedure. Optical properties of treated surface were studied by PL measurements which were performed at 300 K, using excitation of the 514-nm line from an Ar^+ ion laser, working in CW mode. The laser beam was focused on the sample surface by a 10× long-working-distance microscope objective lens to a spot of about 100 μm diameter. The excitation beam power was reduced by a neutral density filter to the value of 15 mW (measured directly before the sample surface), so that the excitation density did not cause the sample heating. The same microscope objective, which focuses the excitation beam on the sample surface, was also utilized to collect PL signal in back-scattering mode. The collected PL signal was then dispersed using a 0.46-m spectrometer equipped with a grating of 600 lines/mm and detected by a multichannel CCD camera cooled to 146 K, which gives a high signal-to-noise ratio. Specific contact resistance was measured by c-TLM method [11].

3. Results and discussion

3.1. VASE analysis

The results of ellipsometric investigations are showed in Tab. 1 and Figs. 1–3. Table 1 summarises details of (100) GaAs surface with thickness and complex index of refraction of resulting surface after different treatments. The values of optical constants are given for λ = 630 nm to allow for their composition with the standard ellipsometric data obtained with the use of He-Ne laser. These results indicate the presence of a modified layer on Ar^+ sputter etched (100) GaAs surface with refraction index n = 3.8–3.9 and extinction coefficient $k \approx 0.4$. Thus, the surface is free from native oxide (n_{ox} = 1.8), though the near-surface is damaged. The refractive index and extinction coefficient for non-damaged GaAs surface (without any treatment) are n = 0.380 and k = 0.208, respectively. The results shown in Tab. 1 confirm that thickness and degree of surface damage increase with an increase in power and sputter etching time. Thus, the best results were obtained by reducing power to P = 70 W and time to t = 30 s, what corresponds to etching rate of 5 nm/min. The characteristic of imaginary part ε_2 of dielectric function is very sensitive to the degree of surface damage. In Fig. 1 we observe the shift of the maximum of the value of ε_2 towards lower energy. Additionally, 3D graph (Fig. 3) shows dependence of ε_2(E):P, t as

T a b l e 1. (100) GaAs surface state after different treatments.

Surface treatment		Spectroscopic ellipsometry (for $\lambda = 630$ nm)			
Ion etching					
Power [W]	Time [s]	Model*	Thickness of superficial layer [nm]	Refractive index n	Extinction coefficient k
250	30	A	$d_1 = 50.00$	3.901	0.400
150	40	A	$d_1 = 40.00$	3.910	0.429
70	20	A	$d_1 = 10.90$	3.828	0.458
70	30	A	$d_1 = 13.52$	3.843	0.456
70	40	A	$d_1 = 13.90$	3.843	0.456
70	90	A	$d_1 = 20.60$	3.854	0.450
Wet etching in 5% HCl; $t = 3$ min		B	$d_2 = 2.02$	1.820	0
•Wet etching in 5% HCl; $t = 3$ min ••Ar^+ ion etching; $P = 70$ W, $t = 30$ s		A	$d_1 = 10.00$	3.702	0.398
Oxide on GaAs		B	$d_2 = 2.15$	1.802	0
GaAs			—	3.839	0.208

*Model A – modified layer on GaAs substrate, model B – oxide layer on GaAs substrate.

a result of difference between the influence of chemical and sputter etching of GaAs surface.

It is a very interesting result in context of fractional-dimensional model application (FDMA) [12]. In particular, this model is very useful to study electron interband optical transitions in the vicinity of van Hove critical points (CP) [13] and when used with spectroscopy, the ellipsometry allows the analysis of the CPs. This analytical--ellipsometric technique extracts the basic information on relevant physical quantities from the observed optical spectra and consequently can characterise damage properties

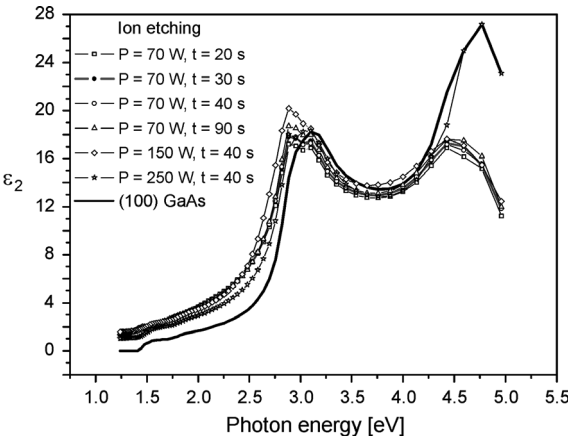

Fig. 1. Spectral characteristics $\varepsilon_2(E)$ of (100) GaAs after Ar^+ sputter etching. Theoretical data of (100) GaAs according to [9].

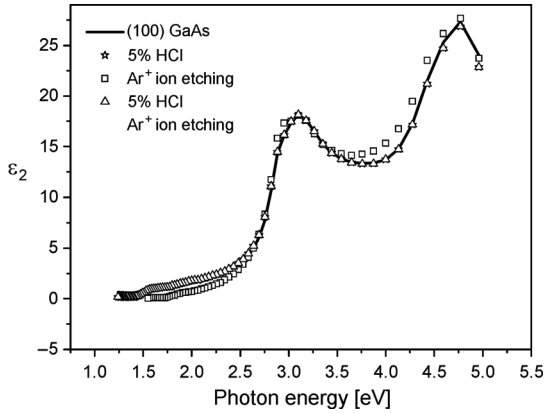

Fig. 2. Spectral characteristics $\varepsilon_2(E)$ of (100) GaAs after different surface treatments. Theoretical data of (100) GaAs according to [9].

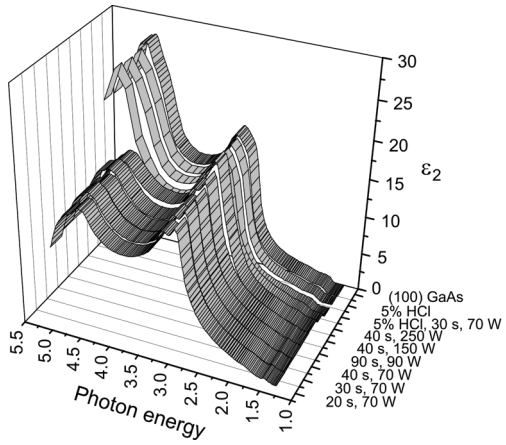

Fig. 3. Spectral characteristics $\varepsilon_2(E)$ of (100) GaAs after different surface treatments. Theoretical data of (100) GaAs according to [9].

of the treated surface. The more detailed analysis of (100) GaAs sputter treated surface will be published in another paper. Ellipsometric results indicate that GaAs surface after chemical etching in 5% HCl is not modified but is characterised by thin (d = 2 nm) oxide layer, whereas two-step treatment: etching in 5% HCl for 60 s followed by sputter etching in Ar^+ plasma at P = 70 W and t = 30 s allows to obtain surface without continuous oxide layer and simultaneously the modification of near-surface region is minimized.

3.2. X-ray photoemission

The influence of different surface treatments on the composition of near-surface region of (100) GaAs is illustrated in Tab. 2 and Figs. 4–6. The main discussion regarding

surface composition and the subsequent changes in the treated surface is related to Ga $2p_{3/2}$, As 3*d* and Ga 3*d* XPS signals. Generally, the XPS results indicate that both Ga and As lines show two chemical states – one at lower binding energies related to GaAs substrate and the second one at higher binding energies related to both gallium and arsenic oxides. For XPS spectra of Ga $2p_{3/2}$ (Fig. 4**a**) the dominant lines come from the oxide – the binding energy (BE) of the fitted line attributed to Ga_2O_3 is E_B = 1118.2–1118.4 eV, depending on the surface treatment. The lower BE line is attributed to pure GaAs. The BE of these lines ranges between E_B = 1117.1 and 1117.4 eV. This value is close to that reported for GaAs (*e.g.*, NIST database). Figures 4**b** and 6 present the results of precise analysis of Ga 3*d* line which can be treated as a core level despite low BE. This line comes from the electrons with much higher kinetic energy than the electrons emitted from the Ga $2p_{3/2}$ sublevel. Thus, due to the energy dependent inelastic electron mean free path, this line represents much

T a b l e 2. Chemical composition of (100) GaAs surface after different treatments.

	Chemical composition of GaAs surface [%]			
	GaAs surface treatment			
Chemical element	Without treatment	5% HCl, t = 3 min	Ar^+ ion etching; P = 70 W, t = 30 s	5% HCl; t = 3min Ar^+ ion etching; P = 70 W, t = 30 s
C	17.6	25.7	32.1	28.3
O	32.1	32.5	21.8	30.3
Ga	20.3	24.2	21.5	20.3
As	21.0	17.6	17.6	21.0
As_2O_3/GaAs	43.2	16.4	10.4	7.6
As/Ga	1.03	0.72	0.81	1.02

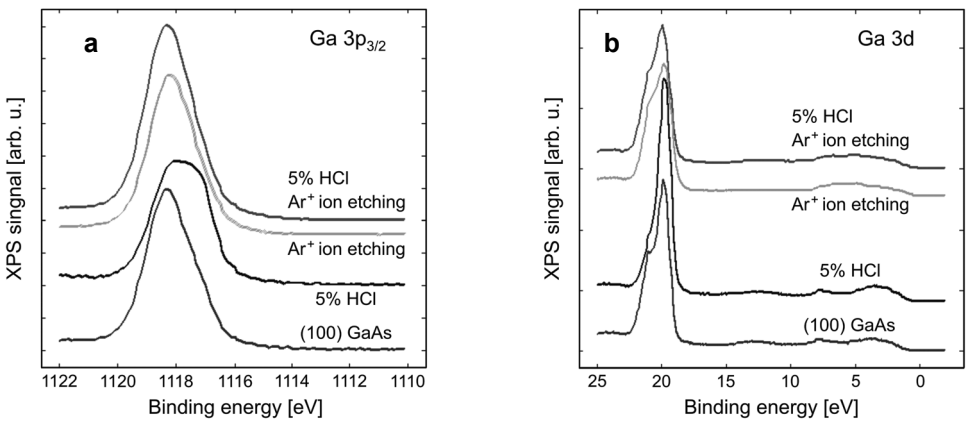

Fig. 4. XPS spectra of Ga $2p_{3/2}$ (**a**), Ga 3*d* and valence band signals from (100) GaAs surface after chemical etching in 5% HCl, Ar^+ ion etching and two-step treatment: chemical etching in 5% HCl, Ar^+ ion etching. Data for non-treated surface are shown for comparison.

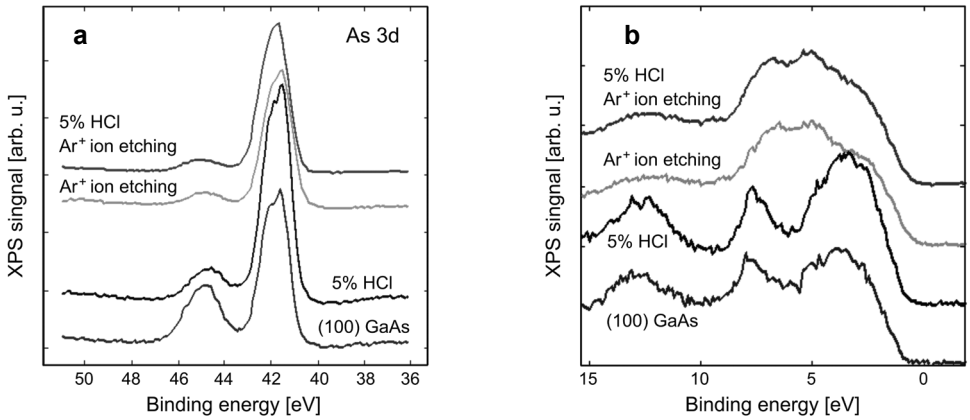

Fig. 5. XPS spectra of As 3*d* level (**a**), and valence band (**b**) spectra from (100) GaAs surface after chemical etching in 5% HCl, Ar^+ ion etching and two-step treatment: chemical etching in 5% HCl, Ar^+ ion etching. Data for non-treated surface are shown for comparison.

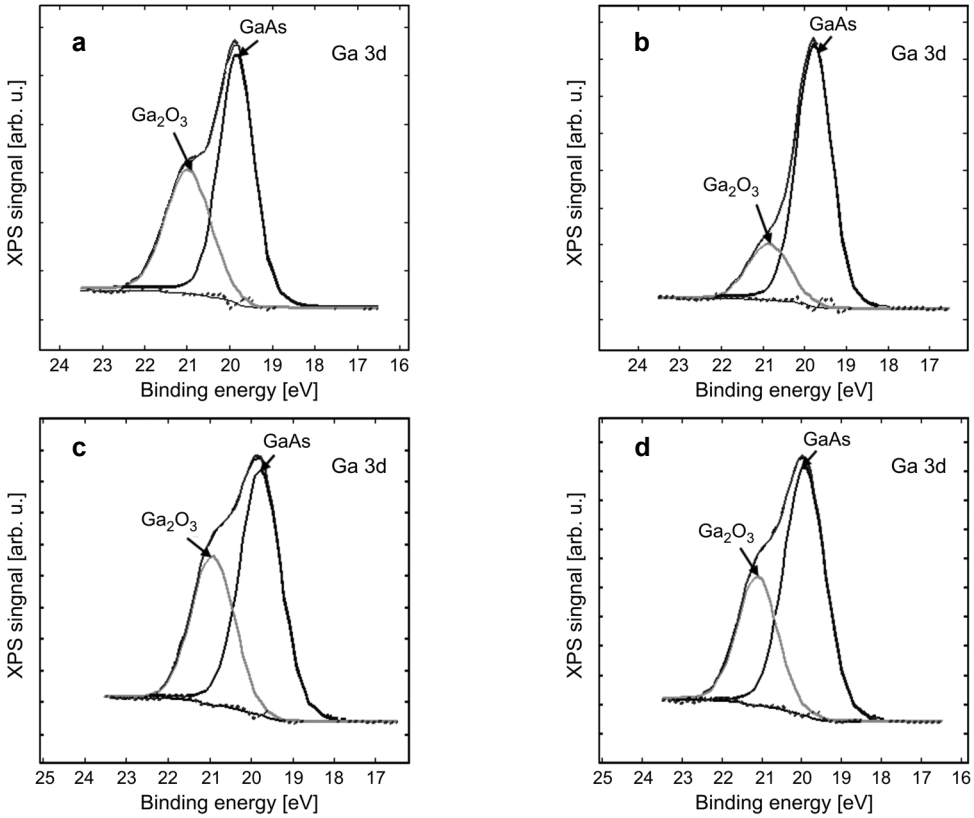

Fig. 6. XPS deconvoluted spectra of Ga 3*d* signal from (100) GaAs surface: without treatment (**a**), after etching in 5% HCl, $t = 3$ min (**b**), after Ar^+ ion etching – $P = 70$ W, $t = 30$ s (**c**), after: etching in 5% HCl, $t = 3$ min and Ar^+ ion etching – $P = 70$ W, $t = 30$ s (**d**).

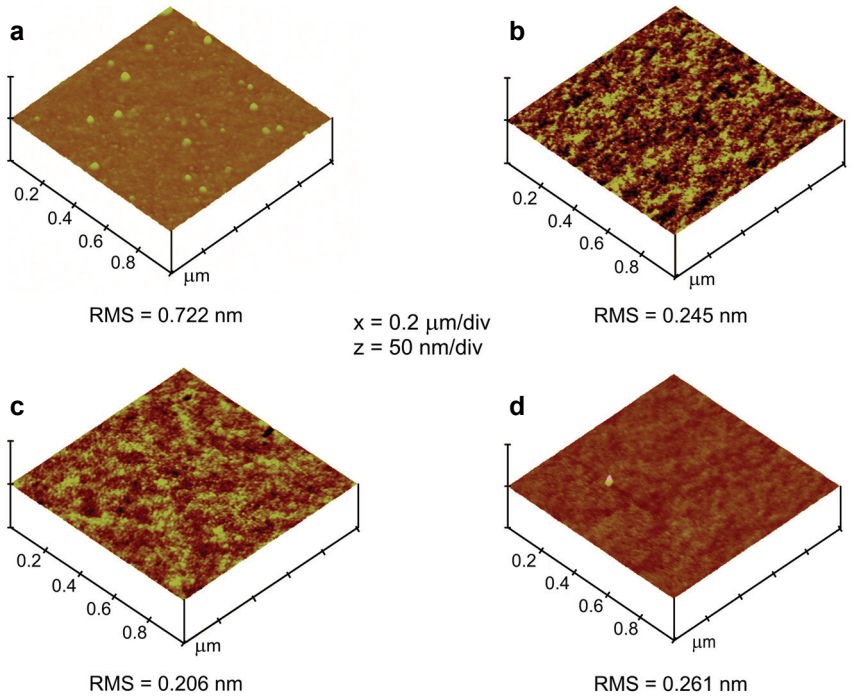

Fig. 7. AFM micrographs of (100) GaAs surface; without treatment (**a**), after etching in 5% HCl, $t = 3$ min (**b**), after Ar^+ sputter etching, $P = 70$ W, $t = 30$ s (**c**), after: etching in 5% HCl, $t = 3$ min and Ar^+ sputter etching – $P = 70$ W, $t = 30$ s (**d**).

more the bulk character of the chemical states. After fitting procedure, one can see that the line at lower binding energy $E_B = 19.9$ eV, which can be attributed to GaAs, has higher intensity than the line at energy $E_B = 21.0$ eV coming from the Ga_2O_3 oxide. For the sample treated in 5% HCl this line is hardly visible, indicating a relatively clean surface with a thin layer of the oxide. Basing on the exponential damping of photoelectron intensity and the energy dependence of the inelastic mean free path (IMFP) (*e.g.*, NIST software), one can estimate the thickness of the oxide film as $d = 1-3$ nm. Such conclusion agrees very well with the elipsometric results. The presented analyses are possible due to the high quality of surface morphology which was detected after chemical and as well sputter treatment obtained from AFM studies (Fig. 7) (RMS ≈ 0.2 nm). The large difference between the structures of the Ga 3*d* and Ga 2*p* XPS lines is a clear indication that the gallium oxide forms only on the top layer of the surface of GaAs. It agrees with the optical properties of the film terminating the GaAs crystal. Arsenic line shows also two chemical states as it is seen in the results of the As 3*d* XPS peaks (Fig. 5**a**). The spin orbit splitting of $E_B = 0.69$ eV and the theoretical branching ratio of the As $3d_{5/2}$ and As $3d_{3/2}$ intensities have been assumed for both main peaks visible at BE of about $E_B = 41.5$ eV and $E_B = 45$ eV. The first doublet with maximum EB at $E_B = 41.4-41.6$ eV originates from the GaAs

whereas the second broader feature at about 45 eV can be attributed to As_2O_3 (*e.g.*, NIST database). The total intensities of two doublets were used to calculate the ratio of two chemical components (As_2O_3/GaAs). A remarkable variation of this ratio has been shown in Tab. 2. Similarly to the Ga 3*d*, the As 3*d* line comes from the relatively fast electrons (with high kinetic energy), so this result reflects the composition within the topmost few nanometers (surface and bulk). One has to remind that the presented measurements have been obtained after a short (t = 20 s) Ar^+ sputter etching of all samples, which removed the surface contamination, but was not able to remove the oxide layers. This result shows that surface after two-step treatment: wet etching in 5% HCl followed by Ar^+ sputter etching is characterised by the thinnest layer of the As_2O_3 phase. The valence band (VB) spectra shown in Fig. 5**b** support the mentioned earlier theses. The observed differences between treated surfaces are remarkable. The main difference is noticed between non-treated and Ar^+ sputtered surface. One can suppose that the broadening and shifting of the VB features towards higher BE are the results of surface defects or even amorphousation caused by sputtering. The results of the surface treatment are reflected in the atomic composition derived from the XPS results. The analysis of the concentration ratio c_{As}/c_{Ga} indicates that chemical and as well sputter etching modify surface stoichiometry, c_{As}/c_{Ga} equals 0.72 and 0.81, respectively. In the experiments of combining chemical etching in 5% HCl and Ar^+ sputter etching (P = 70 W, t = 30 s), the atomic concentration ratio c_{As}/c_{Ga} tends to a stoichiometry one (1.02).

3.3. Photoluminescence and TLM results

Photoluminescence spectra of (100) GaAs surface before and after Ar^+ sputter etching are shown in Fig. 8. Graph on Fig. 8**a** illustrates etching time effect in AXT GaAs

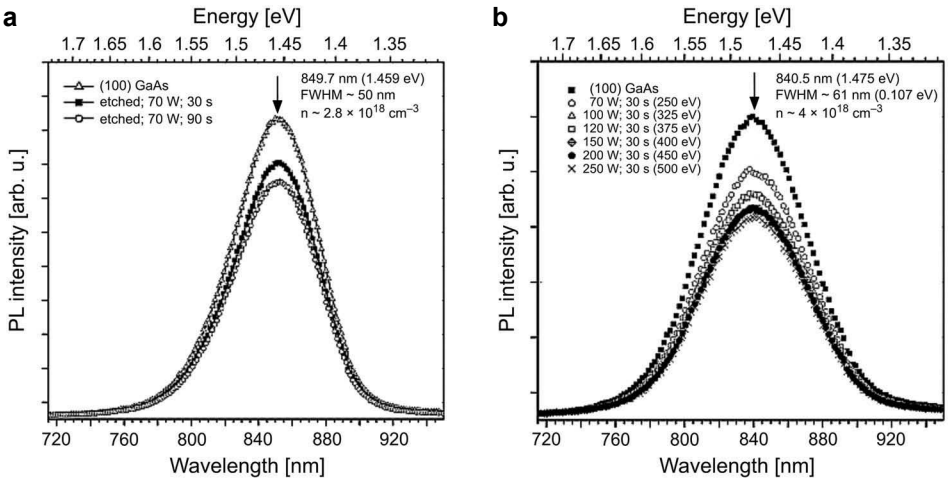

Fig. 8. The dependence of room temperature PL signal of GaAs samples on parameters of Ar^+ ion etching; the influence of etching time (**a**), the influence of the etching beam power (**b**).

T a b l e 3. The specific contact resistance for different GaAs surface treatments.

Surface treatment	Contact resistance [Ωcm^{-2}]	Contact resistance after long-term thermal stability [Ωcm^{-2}]
Without treatment	3.2×10^{-6}	1.7×10^{-5}
Wet etching in 5% HCl; t = 3 min	2.5×10^{-6}	1.1×10^{-5}
Ar^+ ion etching; P =70 W, t = 30 s	1.1×10^{-6}	5.5×10^{-6}
Wet etching in 5% HCl; t = 3 min Ar^+ ion etching; P = 70 W, t = 30 s	3×10^{-6}	2.0×10^{-6}

substrate. Figure 8**b** presents the influence of etching power on the PL signal from GaAs epi-ready substrate. These results indicate that there are no spectral shift of the PL peak position and full width at half maximum (FWHM = 61 nm). However, in both cases PL intensity suppression is observed.

Finally, three investigated procedures have been applied as surface preparation prior Ni/AuGe/Ni/Au ohmic contact deposition. TLM measurements results summarized in Tab. 3 indicate that the ohmic contacts without pretreatment or with only chemical etching in 5% HCl are characterised by poor thermal stability. The best results were obtained for Ni/AuGe/Ni/Au ohmic contact with two-step treatment: etching in 5% HCl followed by Ar^+ sputter etching before metal deposition. As a result of optimization of (100) GaAs surface treatment the lateral uniform and long-term thermal stable ohmic contact was created, with average specific contact resistance $r_c = 2\times10^{-6}\ \Omega\,\mathrm{cm}^{-3}$.

4. Conclusions

Summarising, various procedures of GaAs surface treatments have been developed. Our comparative study shows that the best results are obtained by combining chemical etching in 5% HCl and Ar^+ sputter etching (P = 70 W, t = 30 s). GaAs surface treated by this method was characterised by 10 nm thin modified layer with good morphology and the atomic concentration ratio c_{As}/c_{Ga} tended to stoichiometry one. The measurable results of this work indicate that this procedure is promising as surface treatment for optimised ohmic contact during fabrication of Quantum Cascade Lasers.

Acknowledgements – Authors would like to thank Mr. Wojciech Macherzyński for RTA processing.

References

[1] SIRTORI C., PAGE H., BECKER C., ORTIZ V., *GaAs-AlGaAs quantum cascade lasers: physics, technology, and prospects*, IEEE Journal of Quantum Electronics **38**(6), 2002, pp. 547–558.

[2] KOSIEL K., BUGAJSKI M., SZERLING A., KUBACKA-TRACZYK J., KARBOWNIK P., PRUSZYŃSKA-KARBOWNIK E., MUSZALSKI J., ŁASZCZ A., ROMANOWSKI P., WASIAK M., NAKWASKI W., MAKAROWA I., PERLIN P., *77 K operation of AlGaAs/GaAs quantum cascade laser at 9 μm*, Photonics Letters of Poland **1**(1), 2009, pp.16–18.

[3] KOSIEL K., KUBACKA-TRACZYK J., KARBOWNIK P., SZERLING A., MUSZALSKI J., BUGAJSKI M., ROMANOWSKI P., GACA J., WÓJCIK M., *Molecular-beam epitaxy growth and characterization of mid-infrared quantum cascade laser structures*, Microelectronics Journal **40**(3), 2009, pp. 565–569.

[4] PAPIS-POLAKOWSKA E., *Surface treatment of GaSb and related materials for the processing of mid-infrared semiconductor devices*, Electron Technology: Internet Journal **37/38**, 2005/2006, pp. 1–34.

[5] ZHAO Q., DENG Z.W., KWOK R. W.M., LAU W.M., *Damage of InP (100) induced by low energy Ar^+ and He^+ bombardment*, Journal of Vacuum Science and Technology A **18**(5), 2000, pp. 2271–2276.

[6] GOODMAN S.A., AURET F.D., DEENAPANARY P.N.K., MYBURG G., *Electrical properties of Sc Schottky barrier diodes fabricated on argon-ion sputtered p-GaAs*, Japanese Journal of Applied Physics, Part 2: Letters and Express Letters **37**(1A/B), 1998, pp. L10–L12.

[7] GHITA R.V., NEGRILA C., MANEA A.S., LOGOFATU C., CERNEA M., LAZARESCU M.F., *X-ray photoelectron spectroscopy study on n-type GaAs*, Journal of Optoelectronics and Advanced Materials **5**(4), 2003, pp. 859–863.

[8] WOLAN J.T., EPLING W.S., HOFLUND G.B., *Characterization study of GaAs (001) surfaces using ion scattering spectroscopy and x-ray photoelectron spectroscopy*, Journal of Applied Physics **81**(9), 1997, pp. 6160–6164.

[9] J.A. Woollam Co. Inc. WVASE 32 program v. 3.441, tabulated at UNL (Lincoln University, Nebraska, USA).

[10] MOULDR J.F., STICKLE W.F., SOBOL P.E., BOMBEN K.D., *Handbook of X-ray Photoelectron Spectroscopy*, Physical Electronics, 1995.

[11] REEVES E.H., *Specific contact resistance using a circular transmission line model*, Solid State Technology **23**, 1980, pp. 487–490.

[12] XING-FEI HE, *Fractional dimensionality and fractional derivative spectra of interband optical transitions*, Physical Review B **42**(18), 1990, pp. 11751–11756.

[13] YU ZHAOXIAN, MO DANG, *Property of Van Hove critical points in fractional-dimensional space*, Chinese Physics Letters **10**(7), 1993, pp. 385–388.

Received June 23, 2009